Toughness Enhancement of Nanostructured Amorphous and Semicrystalline Polymers

Goerg H. Michler, Rameshwar Adhikari, Sven Henning*

Institute of Materials Science, Martin Luther University Halle-Wittenberg,
D-06099 Halle/Saale, Germany
E-Mail: michler@iw.uni-halle.de

Summary: An overview is given of different micromechanical deformation processes leading to an enhancement of toughness in heterophase polymers. The well-known mechanism of rubber or particle toughening of semicrystalline polymers was studied in HDPE and PP blends. In particular, the micromechanical processes in the semicrystalline polymer strands between modifier particles were investigated in detail, revealing processes of separation, yielding, breaking and twisting of lamellae. These processes are compared with lamellae forming amorphous SBS block copolymers with alternating soft (polybutadiene) and hard (polystyrene) layers. Depending on the deformation direction, the mechanism of thin layer yielding or chevron formation appears. In both polymeric systems, the initial stage of deformation is characterized by a plastic yielding of the soft phase with a reorganization of the hard (glassy or crystalline) lamellae. The second stage is determined by the alignment of the hard phase towards the deformation direction and the plastic yielding. Detailed comparison of these similar mechanisms in very different polymers with similar nanostructured morphology should help to improve toughening of amorphous as well as semicrystalline polymers.

Keywords: electron microscopy; micromechanical mechanisms; morphology; polyolefins; SBS block copolymers: thermoplastic polymers; toughness enhancement

Introduction

Toughness of polymers is an important property for many practical applications. In this context, the term 'toughness' denotes the absorption of energy during a deformation, which subsequently ends in fracture. The aim of polymer modification is usually to develop a material with a high toughness and a large plastic elongation at break, whilst retaining the desirable properties such as

 DOI: 10.1002/masy.200451005

stiffness and strength. This is possible only by modifying the polymer morphology in such a way as to promote a large number of local energy-absorbing plastic deformation processes on a micro- and sub-micrometer scale.

It has been well known for many years that thermoplastics can be toughened by adding 5-25% of a suitable rubber.[1] This process of rubber toughening is of major importance to the plastics industry. It has proved so effective that the technology has been extended to almost all of the commercial glassy thermoplastics, including polystyrene (PS), poly(styrene-acrylonitrile) copolymer (SAN), polymethyl-methacrylate (PMMA) and polyvinylchloride (PVC). It has also been applied to several thermosetting resins and to semicrystalline polymers, notably polypropylene (PP) and polyamides (PA).

In rubber-toughened, high-impact polymers, the thermoplastic component forms the matrix in which the rubber phase is dispersed as particles. A general disadvantage of this modification is a pronounced decrease in strength and stiffness due to the rubber content. However, a good balance of these properties in combination with other properties (e.g. transparency, flame retardancy) and a good processability is demanded for many applications of polymers. Recently, some new techniques and micromechanical mechanisms were found as alternative toughening mechanisms. An overview of these mechanisms is given in the next section.

Block copolymers allow the control of structure on the nanometer scale and enable the combination of good mechanical properties with other properties such as transparency, recyclability etc. Due to the connectivity of the component chains and their inherent chemical incompatibility, the dissimilar blocks prefer to segregate, which gives rise to a rich variety of ordered structures called microphase separated structures.[2-4] However, the spatial extent of phase segregation is limited by the connectivity of the chains and hence the periodicity of structures lies in the order of the gyration radius (R_g) of the copolymer molecules. Classically, different ordered nanostructures are achieved by changing the overall composition of the copolymer in the two-component block copolymers.

Block copolymers have long been used as compatibilizers in binary polymer blends. Due to their intrinsic transparency, these polymers find application in the preparation of attractive packaging films for foodstuffs. Styrene/butadiene block copolymers can be used as impact modifiers for general purpose polystyrene.

In addition to the variation of the overall composition of block copolymers, the morphology can be adjusted by changing the processing conditions (processing temperature, cooling rate etc. or solution casting using different solvents). Application of external fields such as shearing, electric fields etc. can align the microstructures in a preferential direction leading to anisotropy in their physical properties.[5-9] Another way of adjusting morphology is to assemble the polymer chains in the form of ABC triblocks, giving the copolymer molecules different topologies (linear, star-shaped or grafted chains), and interfacial structures (neat, tapered or statistical transition at the interface), i.e., a wide variety of architectures. For example, in styrene/butadiene systems, the morphology ranges from PB cylinders in a PS matrix, to alternating lamellae and co-continuous structures, and even styrene domains dispersed in a rubbery matrix in a narrow composition range ($\Phi_{PS} \sim 0.70$).[10]

The formation of alternating layers of polystyrene and polybutadiene instead of cylindrical morphology in the sample is associated with its highly asymmetric architecture. A clear deviation from the classical picture of block copolymer phase diagrams can be achieved by the modified molecular architecture.[9, 11-13] The orientation of the microstructures and the occurrence of lamellar structures have a pronounced influence on the mechanical and micromechanical deformation behavior of the block copolymers. The deformation of the lamellar block copolymers is accompanied by a well-defined yield point. After the expansion of the necking zone over the whole tensile specimen (drawing), an orientation hardening begins. In contrast to the whitening of the linear block copolymers having PS matrix during tensile testing, the lamellar star block copolymer shows no stress whitening. Moreover, below a critical thickness of PS lamellae of about 20 nm, a transition from the usual craze-like deformation of PS to a so-called *'thin-layer yielding mechanism'* is observed.[9] This ability of the thin PS lamellae to reveal large homogeneous plastic deformation is considered as a new route of toughening on a nanometer scale.

A better understanding of structure modification and the improvement of mechanical properties is a task of particular scientific and economic importance. Structure, morphology and mechanical properties are linked by the micromechanical processes of deformation and fracture.[14, 15] Recently, smaller structural details have become increasingly important for defined improvement of mechanical properties, with a shift from the details on the micrometer scale to those on the nanometer range. Improved knowledge of the micromechanical processes on these different length scales provides a very direct way of improving mechanical properties.

Micromechanical processes are usually highly localized. Recently, several different techniques have been applied to study micromechanical properties. Besides spectroscopic and scattering techniques, the techniques of electron and atomic force microscopy are particularly useful for direct determination of micromechanical properties of polymers (an overview of these techniques in ref. [1417]). Using special micro-tensile devices for the electron and atomic force microscopes, in situ deformation tests can be performed. Since these techniques also allow the study of morphological details, they enable us to investigate structure-property correlations in a very direct way.

In this work, the toughness enhancement of rubber-modified or particle-modified semicrystalline polymers is discussed in dependence on the plastic yielding processes of the lamellar, semicrystalline matrix parts at and between the modifier particles. These lamellar yielding processes are compared with similar processes in lamellae-forming styrene/butadiene star block copolymers.

Concepts of Toughness Enhancement

There are several different mechanisms by which the toughness of polymers can be enhanced at room temperature or at lower temperatures. Some of them are widely applied in the plastics industry, others are theoretical possibilities.

i. Rubber Particle Toughening (General Modifier Particle Toughening)

Rubber toughened thermoplastics were first manufactured in the late 1940s and have been studied very extensively. Fracture toughness can be increased by up to one order of magnitude by adding a small amount (usually 5-25%) of a suitable rubber or elastomer to the thermoplastics. This effect was initially utilized in PS and SAN by grafting to butadiene rubber, yielding high-impact polystyrene (HIPS) and acrylonitrile-butadiene-styrene copolymer (ABS), respectively. The addition of rubber particles promotes energy absorption through the initiation of local yielding. Fibrillation in both the crazes and the rubber membranes of the 'salami' particles is typical of HIPS; the formation of matrix crazes in combination with dilatational shear bands, where the voids are confined to the rubber phase, is typical of many grades of ABS. Craze-like dilatational shear bands are formed in toughened grades of PVC, PMMA, PP and epoxy resin.[1, 14, 18] Elastomeric particles can be distributed in the matrix in the form of homogenous particles etc. In systems with 'salami' or 'core-shell' particles, hard polymer sub-inclusions occasionally can be deformed by cold drawing ('core flattening') as an additional mechanism of energy absorption.[19]

ii. Particle Filled Polymers (Composites)

Inorganic filler particles with a small interfacial strength yield to debonding and cavitation during loading. The microvoids thus formed act as stress concentrators (like elastomer particles), and can therefore initiate local yielding processes and increase toughness. Preconditions are the particles, which are small enough (including nanoparticles) with a narrow size distribution, with a good separation and optimum distance between the particles in the matrix.[14, 20] Particle filled PP and PE systems are examples of this mechanism.

iii. Rubber Network Yielding

It is often assumed that rubber toughening is synonymous with the addition of rubber particles. However, there is an alternative and also very effective approach to rubber toughening of amorphous polymers, using rubber networks. This method involves small particles of a thermoplastic, e.g., PVC, being embedded in the rubber network to form a honey-comb structure,

with very thin layers of rubber separating the thermoplastic particles. The rubber content is usually kept below 10 vol.-% and the blend might consist, for example, of a rubbery ethylene-vinylacetate copolymer (EVA) matrix encapsulating primary particles of PVC which are ca. 1 μm in diameter. When the rubbery network is stretched, the PVC particles yield and absorb energy. One critical parameter is the thickness of the rubber layers, which should not exceed ca. 30 nm.[14, 21, 22] A disadvantage of these systems and the reason why they are not used in the plastics industry is the sensitivity during processing with destruction of the network and its transformation into the usual rubber particle distribution.[14]

iv. Inclusion Yielding

A deformation mechanism similar to that observed in rubber network blends is 'inclusion yielding', in which stiff thermoplastic particles are distributed in a matrix with a slightly lower yield stress, e.g., SAN particles embedded in a polycarbonate (PC) matrix).[23] Under load, stresses transferred to rigid inclusions via the softer matrix can exceed the yield stress of the inclusions and, therefore, the particles are forced to deform plastically and absorb energy.

v. Thin Layer Yielding Mechanism

In lamellae-forming styrene/butadiene star block copolymers, a large homogeneous plastic deformation of PS lamellae was found instead of the usual crazing mechanism. This effect depends strongly on the thickness of the PS lamellae. Below a critical thickness (of about 20 nm) a transition appears from the usual craze-like deformation to the thin-layer yielding mechanism with a drastic increase of elongation at break of up to 200-300%.[9, 24] This new toughening mechanism based on an effect on nanometer scale yields high impact and transparent polymers. In the case of loading the material not in a parallel direction to the lamellae but in an oblique or perpendicular direction, a modification of the deformation mechanism appears with the formation of so-called chevron-patterns or fir-tree or fish-bone patterns, which are described in this work.

vi. Self-Reinforcement

It is well known that strong orientation of the macromolecules increases stiffness and strength of

thermoplastic polymers, e.g., PP and PE.[25] Relaxation processes during cooling demand a fast solidification[26] or the preparation only of thin films or fibers. Using special compaction techniques, bulk material can be produced from these films or fibers with good toughness at a high level of stiffness and strength.[27, 28]

vii. Phase Transformation

Following a concept of toughening of ceramic materials due to the phase transformation mechanism, a theoretical estimation shows that a stress induced transformation from one crystalline phase into another one (e.g. transition from β- to α-crystals in iPP) could absorb energy.[29] However, as yet, there is no experimental confirmation of this mechanism in polymers.

Experimental

Materials and Sample Preparation

Three different kinds of elastomer-modified semicrystalline polymers were used:

- A binary blend was prepared by melt blending of a high-density polyethylene (HDPE) with an elastomer (a very low density PE, VLDPE) in a wt.- ratio of 80/20. The blend was mixed in a Brabender Plasticorder PL 2000 at 180 °C and 40 rpm for 8 min before being pressed to form plates.[30]

- HDPE and 10 wt.-% of a rubber (a stabilized blend of a SB rubber and natural rubber) was mixed in an extruder and prepared as thin films.

- Another rubber-modified sample used was a commercial reactor blend of PP containing 15 vol.-% ethylene-propylene block copolymer (EPR) from PCD Polymers, Linz.

To study the deformation processes in the semicrystalline lamellar matrix in more detail, β-nucleated isotactic polypropylene (Daplen BE 60, Borealis AG, Linz) was used. 1 mm thick sheets were produced using a hot press and subsequently a multistage crystallization procedure.

Lamellae forming asymmetric styrene/butadiene block copolymers (number average molecular weight ~ 100 000 g/mole and total styrene volume content of 0.74) were investigated. For the detailed analysis of lamellar systems, blends of lamellar star block copolymer and polystyrene homopolymer (number average molecular weight ca. 80 000 g/mole) having wide molecular weight distribution were studied (details on the materials used are in refs. [9, 11-13]). The investigated materials supplied by the BASF Aktiengesellschaft, Ludwigshafen were prepared by injection molding (mass temperature 250 °C and mould temperature 45 °C) and solution casting using toluene as solvent.

Techniques

Morphology: To study the morphology of the materials used, ultrathin sections were prepared by ultramicrotomy, or in selected cases by cryo-ultramicrotomy. The thin sections were examined by conventional 100 – 200 kV transmission electron microscopy (TEM). Selective staining using heavy metal compounds such as ruthenium tetroxide (RuO_4) or osmium tetroxide (OsO_4) was generally employed.

Micromechanical testing: To investigate deformation micromechanisms, several different methods were used in this programme:

- Deformation in a commercial tensile tester and studying in a scanning electron microscope (SEM). In order to obtain planar and flat surfaces, the deformed miniaturized tensile bars were epoxy embedded and microtomed down to the middle section of the bar using a Leica microtome with a metal blade. The surface layers (influence of skin morphology, scratches) were thus eliminated. Regions of interest corresponding to the different states of deformation were selected for SEM investigations. Subsequently, a modified permanganic etching technique according to Olley and Bassett[31] was applied to reveal the nanostructure of the deformed material. To avoid electrical charging, samples were sputter coated with a gold layer of 12 nm. Micrographs of the deformation structures were recorded using a Jeol JSM 6300 scanning electron microscope operated at 15 kV accelerating voltage.

- Preparation of 0.5 – 2 μm thick semi-thin sections from the bulk materials followed by

deformation in a special tensile stage fitted to a 1000 kV high-voltage electron microscope (HVEM, in cooperation with Max Planck Institute of Microstructure Physics in Halle/S.) or in a tensile stage for the atomic force microscope (AFM).

- Preparation of ultrathin sections for deformation in a straining device attached to a 200 kV TEM, which also has facilities for cooling and heating the specimen.

Details of the different electron microscopic techniques are given in ref. [16, 17]

Tensile Testing: Tensile testing according to ISO 527 was performed at room temperature (23 °C) using a universal tensile machine at a crosshead speed of 50 mm/min. Some of the specimens were tested using miniaturized dumbbell-shaped tensile specimens by means of a Minimat miniature materials testing device (Polymer Laboratories, UK) at a crosshead speed of 1 mm/min at room temperature.

Results and Discussion

Elastomer modified HDPE

The morphology of the blend HDPE/VLDPE (weight ratio 80/20) is shown in a 200 kV TEM micrograph of an ultrathin section in Figure 1. The dark image structures are caused by selectively stained areas of the specimen by ruthenium tetroxide. On the one hand, they show the amorphous areas between the bright crystalline lamellae with an additional contrast. On the other hand, the dark areas of a few 100 nm in diameter result from strongly stained segregated particles consisting of the elastomeric blend component. Within the accuracy limit of the measurement, the result matches the weight ratio of the 80/20 (corresponding to the volume ratio) quite well. It is typical that a few particularly thick crystalline lamellae of the matrix PE penetrate into the segregated elastomeric particles.

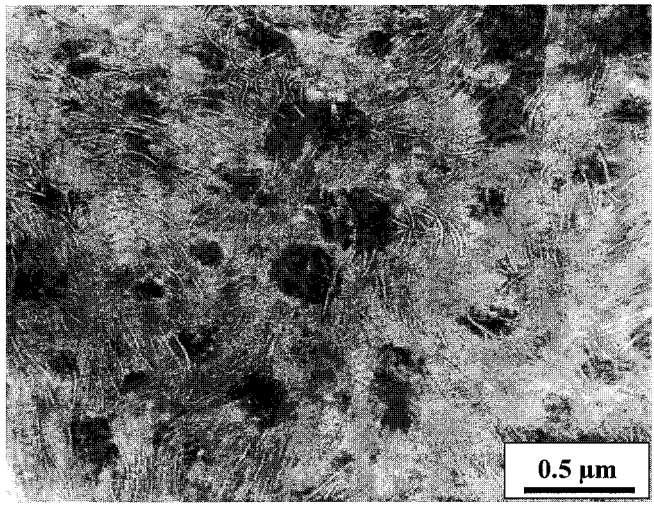

Figure 1. TEM micrograph of a selectively stained ultrathin section of the blend HDPE/VLDPE (weight ratio 80/20).

Using tapping mode in AFM, the specimen morphology in the surface region can be studied without any chemical staining, as shown in Figure 2. Due to their elastomeric properties, the segregated particles appear bright and can be clearly distinguished from their surroundings comprising crystalline HDPE lamellae. Comparison of Figure 1 and Figure 2 reveals a segmental appearance, like beads on a string, in the dark crystalline lamellae in AFM micrograph of Figure 2. Figure 3 shows the image in the original state (1) and images of three steps of the tensile test (2-4), corresponding to average local strains of 8, 16, and 56%. To illustrate the local strain distributions within the imaged (marked) area, four locations a, b, c, d are marked by arrows. While the length of segment ***a*** (near the polar regions of elastomeric particles) does not change, the length of segment ***b***, which is located directly at an elastomeric particle (in the equatorial stress concentration zone), increases significantly. The corresponding local strain (at the three deformation steps) was determined to be 16%, 30% and 146%, respectively. This means that the local strain at position ***b*** is much higher than the average strain. Segments *c* and ***d*** are arranged in the matrix strand between elastomeric particles with a lower stress concentration. Therefore the

local strain is only slightly increased (8, 16, 69%, respectively).

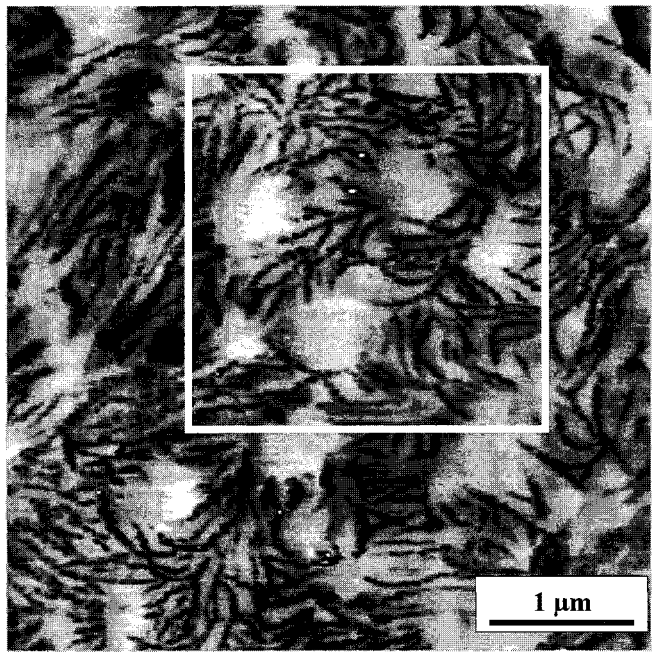

Figure 2. Tapping mode AFM phase image of the HDPE/VLDPE blend with the area marked chosen for studying the micromechanical behavior of the blend.

The sequence of micrographs in Figure 3 represents a true in situ deformation test and illustrates the stress concentration effect at elastomeric particles. Besides the general effect of locally increased plasticity of the matrix strands between particles as the main energy absorbing and toughening effect, additional details of the yielding process are detectable. The area between the dotted lines in Figure 4a is deformed into the whole area visible in Figure 4c in the direction of tensile stress σ, corresponding to a mean strain of about 35%. The comparison of Figure 4a and 4c reveals the deformation behavior of the crystalline lamellae. The lamellae composed of crystalline blocks (like beaded strings) can be detected more easily in Figure 4b and 4d after additional image processing with a high pass filter.[30]

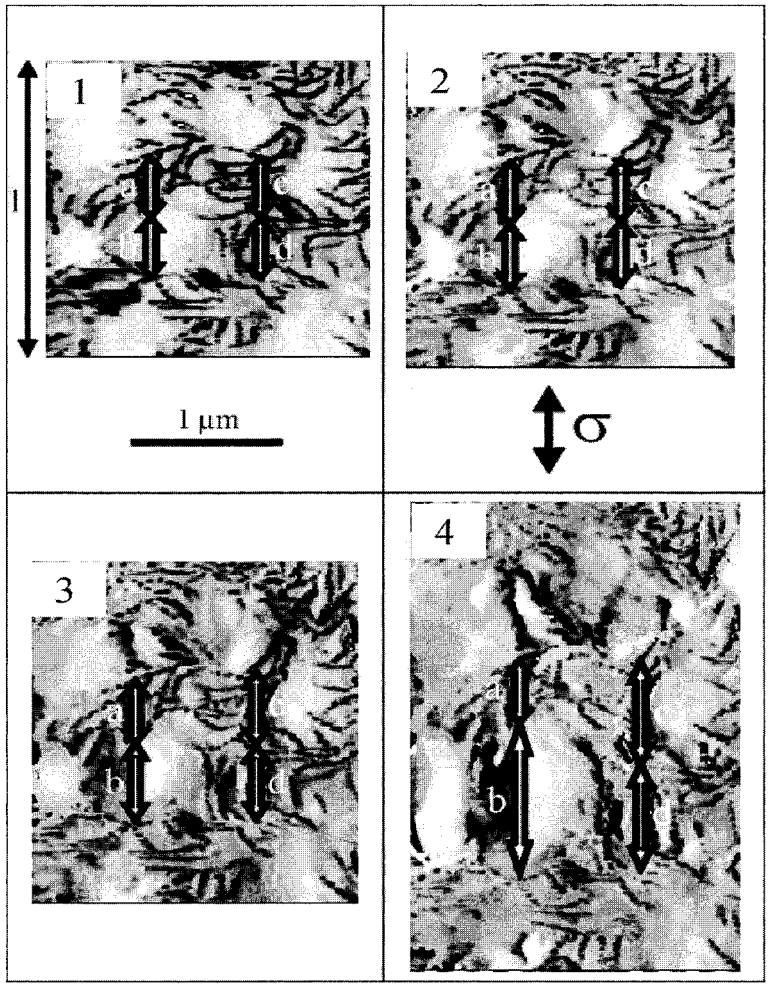

Figure 3. Micromechanical processes in the marked area of Figure 2 shown by tapping mode AFM phase micrographs showing the specimen areas before deformation (1) and in the three stages of an in situ tensile test (2-4).

The typical behavior of lamellae is illustrated by selected lamellae segments marked by capitals at their endpoints. Initially, the lamella segment between AB is nearly perpendicular to σ. During the deformation, it rotates towards the stress direction by an angle of about 14° without changing

the segment length. In contrast to that, the lamella segment CD and also the neighboring parallel lamella segment on the left are already oriented in the stress direction. Owing to the stretching of the lamellae the crystal blocks are separated from one another. The typical behavior of lamellae under stress results from the combination of both effects described. A lot of lamellar segments show rotation towards stress direction as well as additional stretch. This is illustrated by the lamella segment between E and F, which is located in the immediate vicinity of an elastomeric particle. This means that the interfaces between the blocks are the weakest points in the lamellar structure and show a preferred deformation with separation of the microblocks.

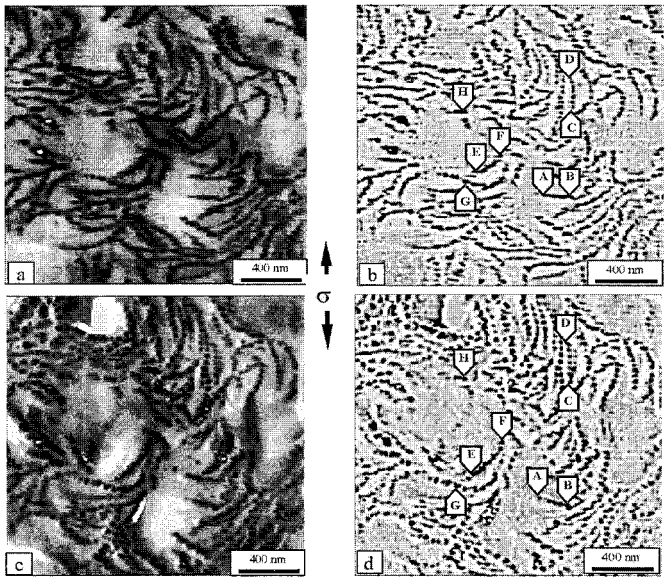

Figure 4. Tapping mode AFM images of the same area of the HDPE/VLDPE blend before deformation (a, b) and after deformation (c, d); pictures on the right (b, d) were produced by additional image processing of the original phase signals (a, c) with a high pass filter.

Pronounced twisting of lamellae is also detectable in the HDPE/rubber blend (see Figure 5). Around the rubber particles the crystalline HDPE lamellae are arranged in nearly perpendicular direction to the particle matrix interface and the extrusion direction MR – Figure 5. After deformation in the MR direction the longer lamellae are broken into shorter pieces, which are

twisted into deformation direction, forming fir tree-like or chevron patterns – Figure 5b.

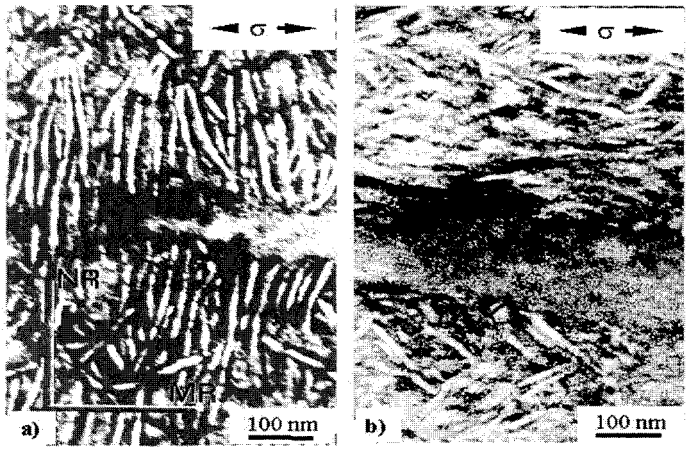

Figure 5. Deformation structures in a HDPE/rubber blend: a) Extension ratio $\lambda = 1$: starting morphology with lamellae in perpendicular direction to extrusion MR; b) $\lambda = 6$: pieces of broken lamellae, twisted and oriented into deformation direction MR, forming fir-tree-like patterns; (NR – normal direction, MR – extrusion (machine) direction and deformation direction, stained thin sections in TEM).

Toughness enhancement of the blends is determined due to local stress concentration at and between the rubber particles and due to the yielding behavior of matrix strands between the particles. This yielding behavior is decisive for the toughening effect. The same mechanism of breaking, separation and twisting of lamellae can also be found during deformation of homo-PE[32] and β-nucleated iPP. These results correspond also with former findings about the deformation processes in HDPE at higher deformation temperatures below the melting point, revealing a greater number of defect layers or smaller crystalline microblocks inside lamellae oriented in parallel direction to the deformation direction.[33]

β-Modified Polypropylene

The special arrangement of the crystalline lamellae and interlamellar amorphous material in a parallel manner in β-iPP (stacks) can be interpreted as a lamellar nanostructure (10 to 20 nm)

consisting of soft (amorphous) and hard (crystalline) components that are interconnected by tie molecules and entanglements. The characteristic deformation structures in β-iPP are shown in the electron micrographs in Figure 6.

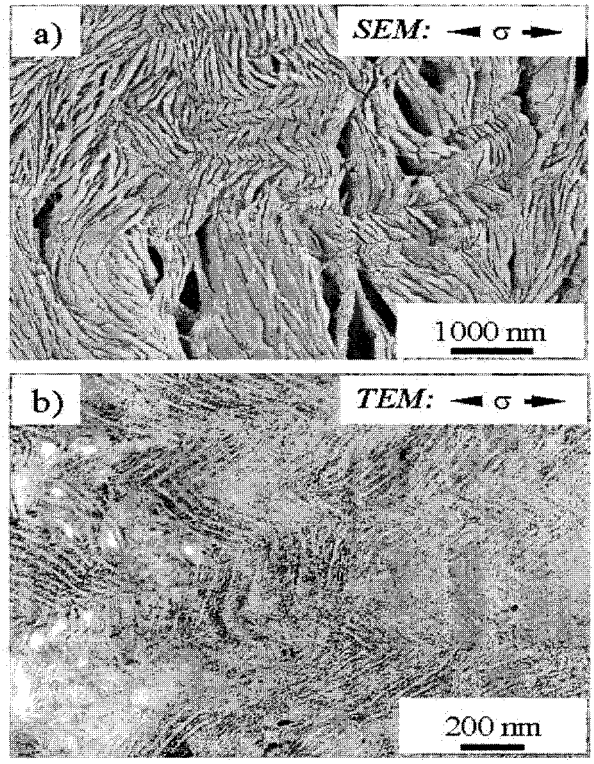

Figure 6. Chevron structures of tilted and separated lamellae in a β-iPP at the early stage of deformation in direction of arrow: a) surface after permanganic etching in SEM and b) thin section after RuO_4 staining in TEM, deformation direction is shown.

A SEM micrograph of the deformed β-iPP (close to the necking region) is given in Figure 6a, where the straining direction is perpendicular to the direction of the lamellar stacks. In the initial stages of deformation ($\lambda \approx 1.2$), two main types of plastic processes can be distinguished. The formation of chevron-like morphology (zig-zag pattern) due to collective twisting of lamellar

stacks and a lamellar separation process are observed simultaneously. Whereas the former process does not include a change in sample volume, the latter is accompanied by intensive microvoid formation and fibrillation within the amorphous portion that can be interpreted as a craze-like deformation mechanism (details in Figure 6b). From the measurement of average lamellar thickness it was concluded that in the initial deformation stage represented here, the crystalline lamellae (appearing as white strands in the TEM micrograph in Figure 6b) remain intact. The simultaneous processes of chevron formation and lamellar separation are controlled by the mobility of the interlamellar, amorphous portion of the material. Additional details about this mechanism can be studied using amorphous lamellar styrene/butadiene block copolymers, in which the thickness of PS and PB lamellae lies in the range of 10-20 nm (see below)

SBS Block Copolymers

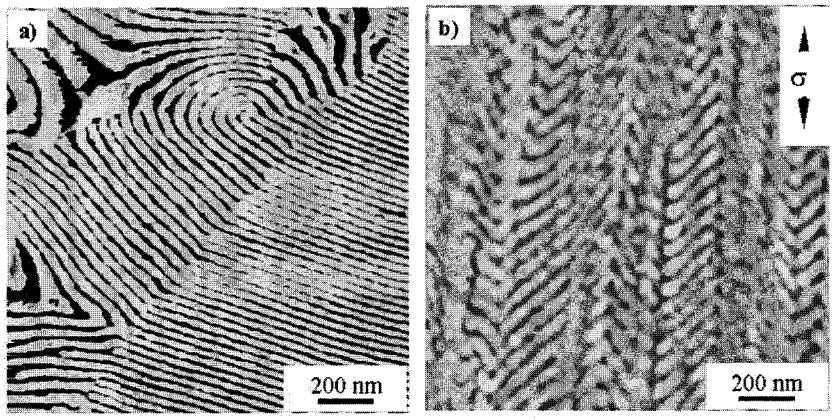

Figure 7. AFM phase images showing the morphology of a solution-cast lamellar SBS triblock copolymer: a) without deformation and b) after deformation, perpendicular direction to lamellae arrangement; cryo-microtomed surface imaged in tapping mode.

It is known that the mechanical and micromechanical properties of block copolymer systems are strongly affected by the type, dimension and orientation of the microstructures. Additionally, the micromechanical response of these materials is influenced by the loading direction relative to the orientation of the microphase-separated structures.

If the material is loaded perpendicular or at an angle to the lamellar orientation direction, the lamellae are folded in a fish-bone-like arrangement (chevron morphology). The morphology of a lamellar SBS triblock copolymer film cast from solution is shown before and after deformation in AFM phase images, Figure 7. After deformation, the regions where the lamellae were initially perpendicular to the strain direction turn into so-called 'chevron morphology' or fish-bone morphology (zig-zag pattern).

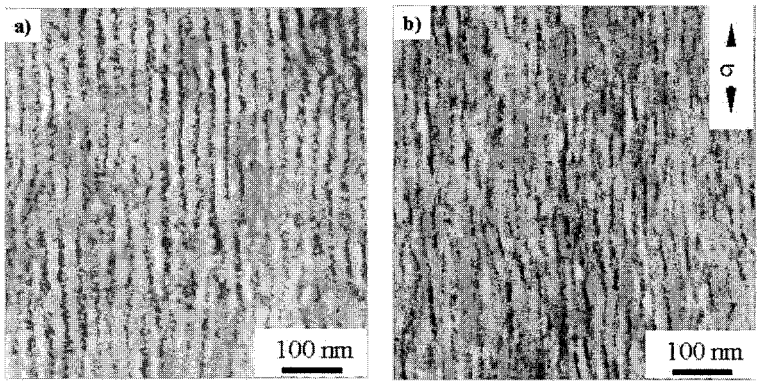

Figure 8. Representative TEM images showing the morphology of an injection molded lamellar SBS triblock copolymer: a) without deformation and b) after deformation in parallel direction to lamellae arrangement; thin section selectively stained by OsO_4.

A different picture appears if the samples are loaded in such a way that the lamellae are parallel to the deformation direction. Figure 8 shows the morphology of an SBS star block copolymer before and after tensile deformation along the injection direction (or lamellar orientation direction). In the undeformed sample, the thickness of the PS lamellae and the lamellar spacing lies in the range of 20 nm and 42 nm, respectively, (Figure 8a). The tensile deformation parallel to the injection direction (i.e., the lamellar orientation direction) led to an extreme plastic drawing of both PS and PB lamellae, (Figure 8b). In the deformed sample the thickness of the PS lamellae and the lamellar spacing have been reduced to about half of their values before deformation. It is worth mentioning that the lamellae were stretched to a very high degree without any cavitation or microvoid formation. In contrast to the diblock copolymers, where the deformation localisation in

the craze-like zones is the principal deformation mechanism,[34, 35] no local deformation bands were observed.

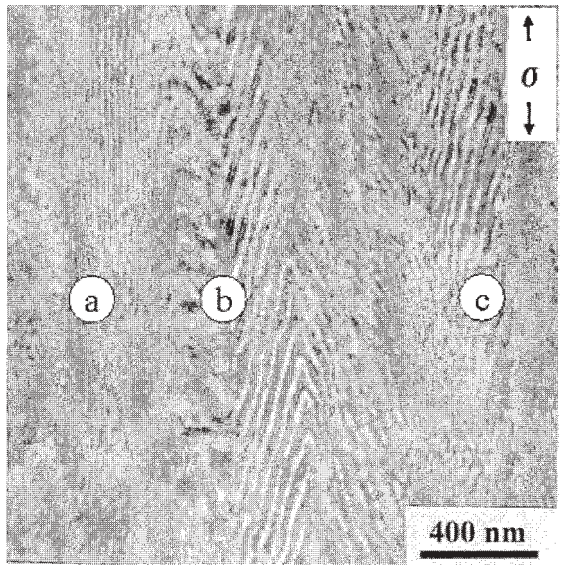

Figure 9. TEM micrograph showing the deformation structures in a lamellar star block copolymer prepared by solution casting, strain direction is shown by an arrow; osmium tetroxide staining.

A summary of the deformation processes illustrated in Figure 7 and Figure 8 is collected in a TEM image of a solution-cast star block copolymer in Figure 9. If the deformation direction is perpendicular or oblique to the lamellar orientation (regions **b** and **c** in Figure 9), different mechanisms may act simultaneously or consecutively. Firstly, a shift of adjacent lamellae (gliding process) occurs. Thereafter, the lamellae break into smaller domains, rotating towards the loading direction. Finally, chevron-like or fir-tree like morphologies are formed. Formation of chevron morphology under mechanical loading was recently reported in oriented lamellar block copolymer samples subjected to tensile deformation perpendicular to the lamellar alignment [6]. It should be noted that the thickness of PS lamellae (about 20 nm) remains practically unchanged

in the chevron folded structures after deformation. However, the lamellar long period is increased due to widening of the PB lamellae in the folded 'hinges'. Moreover, the thickness reduction of the PB layers during the parallel deformation was found to be more pronounced. These observations indicate that the rubbery phase reacts earlier towards the applied stress, which was further supported by Fourier transform infra red (FTIR) spectroscopy results.[36]

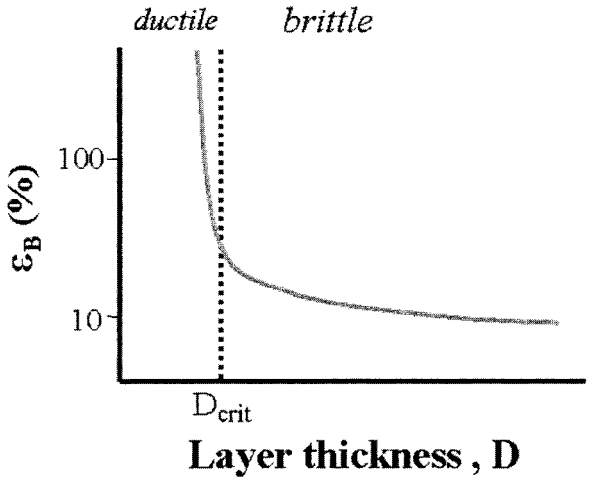

Figure 10. Scheme showing the principal of thin layer yielding mechanism.

If the deformation direction is parallel to the lamellar orientation, a homogeneous plastic yielding of both PS and PB lamellae is detectable (region **a** in Figure 9). Apparently there is no change in the phase morphology besides a significant reduction of the layer thicknesses and the long period (compare different regions in Figure 9). The lamellae are strongly aligned towards the strain direction and the well-defined lamellar structure is even partly destroyed. The large plastic deformation of the glassy PS lamellae under tensile strain found in the star block copolymer studied is in line with the results reported earlier by Kawai et al., who observed a co-operative, drawing, shearing and kinking of the block copolymer microdomains.[37]

From the reduction of the lamellar spacing and the thickness of the PS lamellae in the

undeformed and deformed samples, a local deformation of about 300 % can be estimated. This is the same order of magnitude as the craze fibrils stretching in the crazes of PS (craze fibril extension ration, $\lambda = 4$ [14, 38]). In other words, the yielding of the lamellae in the star block copolymer is analogous to the drawing of craze fibrils in the polystyrene homopolymer.

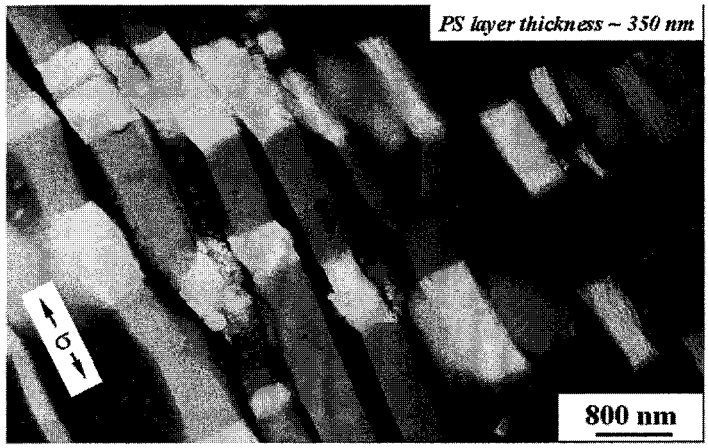

Figure 11. TEM image of a blend consisting of an SBS triblock copolymer and standard polystyrene (20/80 by weight) after deformation; the crazes are exclusively localized in the PS layers; deformation direction is shown.

The polymers designed to form the layered structures (e.g. alternating glassy and rubbery layers in the block copolymers) may undergo homogeneous plastic deformation even without forming any localized deformation zones. This behavior endows the polymers, which are otherwise brittle in the bulk state (e.g., bulk polystyrene), with a ductile property. This mechanism of homogeneous plastic deformation of PS lamellae (thin PS layers) together with adjacent PB lamellae can be described by a new deformation mechanism called '*thin layer yielding*',[9] which is schematically represented in Figure 10. This effect appears if the thickness of the PS layers lies below a critical thickness (D_{crit}). This critical thickness is comparable to the maximum craze fibril thickness in polystyrene homopolymer, i.e., in the range of 20 nm. The difference between the craze fibril yielding and the yielding of the PS lamellae lies in the fact that the craze fibrils stretch between microvoids while the PS lamellae undergo yielding between PB lamellae. Thus, in this case, the

PB lamellae act similar to microvoids in PS crazes and do not hinder the plastic deformation of the glassy polystyrene layers.

The large plastic deformation of the glassy lamellae at room temperature under tensile loading conditions is limited to lamella thickness below a critical value. The deformation mechanism changes from homogeneous drawing of the lamellae to the formation of local craze-like zones when the average thickness of the PS lamellae increases to about 30 nm.[24] The TEM image in Figure 11 illustrates, for example, in a blend of an SBS triblock copolymer and polystyrene homopolymer, how the thickness of the glassy layers affects the deformation micromechanism. Here, the PS layer thickness (average thickness ~ 350 nm) clearly exceeds the critical value, showing only fibrillated crazes inside. These results provide additional evidence for the '*thin layer yielding*' mechanism.

Comparison of Micromechanisms

Similar micromechanisms are observed in two entirely different classes of materials (PP and PE versus block copolymers), which result from their comparable morphologies (lamellar arrangement of the nanostructures). Depending on the loading direction relative to the lamellar alignment, different micromechanisms exist - as shown schematically in Figure 12. In the semicrystalline polymers, when loaded parallel to the lamellar orientation direction, an interlamellar gliding with plastic yielding of the amorphous layers between the lamellae and separation of the lamellae into smaller crystalline fragments with chain unfolding appear, leading to the formation of microfibrils at very high deformation. On the other hand, the mechanism of '*thin layer yielding*' dominates. In lamellar SBS block copolymers, interlamellar gliding is followed by plastic yielding of the butadiene and styrene lamellae corresponding to the "*thin layer yielding*" mechanism.

When loaded perpendicular to the lamellar orientation direction, similar deformation structures are formed both in the semicrystalline polymers (β-iPP and HDPE) and the lamellar SBS block copolymers, i.e., formation of chevron structures. In HDPE and also in β-iPP cavitation and fibrillation in the amorphous phase occur at larger deformation

The high plastic deformation of the amorphous region (including the formation of fibrillated crazes) in iPP leads to a high ductility of the sample. The special morphology of the β-form of iPP yields to a greater toughness than that of the α-form. The parallel array of crystalline lamellae enhances the local interlamellar shearing (if the lamellae are parallel to the loading direction) and lamellar separation and crazing of the amorphous phase (if the load acts perpendicular to the lamellar orientation direction). Since the amorphous region contains a number of defects (such as chain ends) it is more prone to cavitation, leading to the fibrillated crazes. The absence of microvoids in the soft phase of the SBS block copolymers is a most striking difference. The butadiene phase covalently bonded to the styrene chains (no molecular defects) allows cavitation only after the chain scission.

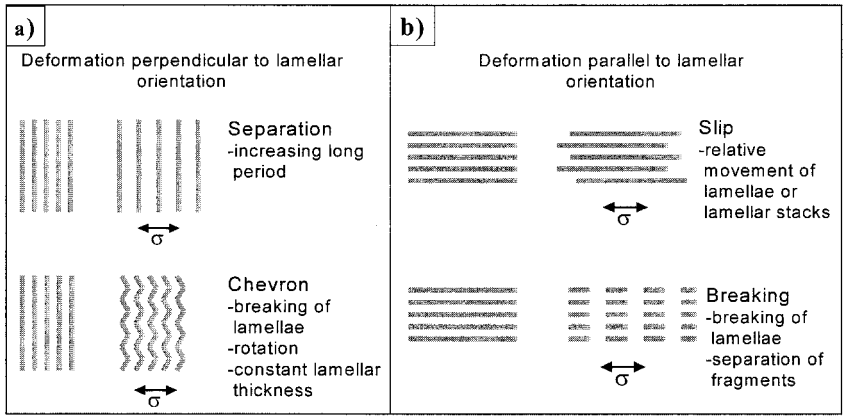

Figure 12. Scheme of micromechanical processes observed in lamellar systems investigated: a) lamellae perpendicular to the strain direction and b) lamellae parallel to strain direction.

Conclusions

Rubber toughening of amorphous and semicrystalline polymers is of major importance to the plastics industry. The basic effects are stress concentration at the particles and initiation of plastic

yielding at and between the particles. In the past, enhancement of the toughening effect was achieved via optimization of the rubber particle size or the inter-particle distance. Up to now, an improvement of the yielding behavior of the matrix itself has not been discussed. Comparison of the micromechanical behavior of semicrystalline polymers (HDPE, iPP) with that of lamellae-forming amorphous SBS block copolymers revealed several similarities. These can be used to improve yielding ability of the semicrystalline matrix strands between the modifier particles. Aspects of particular interest in this sense are:

- The soft interlamellar phase is decisive for the process of interlamellar yielding (if deformation direction is parallel to the lamellae orientation) or twisting, reorganization and chevron formation of the crystalline lamellae (if deformation direction is perpendicular to the lamellar arrangement).

- A controlled cavitation inside the amorphous interlamellar phase can improve the lamellar orientation processes.

- Intense plastic yielding of the crystalline lamellae itself is assisted by breaking of lamellae into shorter crystalline blocks and transformation into microfibrils.

The micromechanical behavior of lamellae-forming heterophase polymers (based on semicrystalline polymers and amorphous block copolymers) has been comparatively studied. It is concluded that the deformation mechanisms of a nanostructured heterophase polymeric system may be dictated by the nature and arrangement of these structures. The basic mechanisms show two stages. The initial stage is characterised by a plastic deformation of the soft phase with a reorganisation of the hard (glassy or crystalline) lamellae. The second stage is determined by the alignment of hard phase towards the deformation direction and plastic yielding. In this way, the knowledge gained using a set of polymers may be used to understand the deformation mechanisms of another set of polymers with comparable phase morphology.

Additionally, the homogeneous plastic flow of glassy phase (i.e. *"thin layer yielding"*) in the lamellar block copolymer has been studied in detail. The significance of this mechanism from a

practical point of view may be found in the fact that it can be used as an alternative toughening mechanism in other brittle polymers.

Acknowledgements

The authors thank Dr. S. Rudolf and Dr. Giesemann, Institute of Macromolecular Chemistry at the Martin Luther University Halle-Wittenberg, for providing the PE blends; Borealis AG, Linz for supplying PP samples and BASF Aktiengesellschaft for the block copolymers. They also thank Prof. U. Gösele, Max-Planck-Institute of Microstructure Physics in Halle/S, for access to the 1000 kV high-voltage electron microscope. We are indebted to the Deutsche Forschungsgemeinschaft (DFG) for financial support. SH and RA acknowledge the research grants from the Max-Buchner-Forschungsstiftung.

[1] C. B. Bucknall, *"Toughened Plastics"*, Applied Science Publishers, London 1977.
[2] S. Bates, G. H. Fredrickson, *Phys. Today* ***1999***, *2*, 32.
[3] I. W. Hamley, "*The Physics of Block copolymers*", Oxford Science Publications, Oxford 1998.
[4] H. Hasegawa, T. Hashimoto, in "*Comprehensive Polymer Science, Suppl. 2*", S. L. Aggarwal, S. Russo Eds., p. 497, Pergamon, London 1996.
[5] A. Keller, J. A. Odell, in: *"Processing, Structure and Properties of Block Copolymers"*, M. J. Folkes, Ed., p 29, Elsevier Applied Science Publishers, London 1985.
[6] Y. Cohen, R. J. Albalak, G. J. Dair, M. S. Capel, E. L. Thomas, *Macromolecules* **2000**, *33*, 6502.
[7] A. Böker, H. Elbs, H. Hänsel, A. Knoll, S. Ludwigs, H. Zettl, V. Urban, V. Abetz, A. H. E. Müller, G. Krausch, *Phys. Rev. Lett.* **2002**, *89*, 135502.
[8] C. C. Honeker, E. L. Thomas, R. J. Albalak, D. A. Hadjuk, S. M. Gruner, M. C. Capel, *Macromolecules* **2000**, *39*, 9395.
[9] G. H. Michler, R. Adhikari, W. Lebek, S. Goerlitz, R. Weidisch, K. Knoll, *J. Appl. Polym. Sci.* **2002**, *85*, 683.
[10] R. Adhikari et al. in this volume
[11] R. Adhikari, G. H. Michler, T. A. Huy, E. Ivankova, R. Godehardt, W. Lebek, K. Knoll, *Macromol.Chem.Phys.* **2003**, *204*, 488.
[12] K. Knoll, N. Nießner, *Macromol. Symp.* **1998**, *132*, 231.
[13] R. Adhikari, R. Godehardt, W. Lebek, R. Weidisch, G. H. Michler, K. Knoll, (**2001**), *J. Macromol. Sci.: Polym. Phys.* **2001**, *40*, 833.
[14] G. H. Michler, *"Kunststoff-Mikromechanik: Morphologie, Deformations- und Bruchmechanismen"*, Carl Hanser Verlag, München 1992.
[15] G. H. Michler, *J. Macromol. Sci.: Polym. Phys.* **1999**, *38*, 787.
[16] G. H. Michler, *Trends Polym. Sci.* **1995**, *3*, 124.
[17] G. H. Michler, *J. Macromol. Sci.: Polym. Phys.* **2001**, 40, 277.
[18] C. B. Bucknall, in: "*Polymer Blends: Vol. 2 – Performance*", D. R. Paul, C. B. Bucknall Eds. P. 83, John Wiley & Sons, New York 2000.
[19] G. H. Michler, C. B. Bucknall, *Plastics, Rubber and Composites* **2001**, 30, 110.
[20] G.-M. Kim, G. H. Michler, *Polymer* **1998**, *39*, 5699.
[21] G. H. Michler, K. Gruber, *Plaste & Kautschuck* **1976**, *23*, 496.

[22] G. H. Michler, *Polymer* **1986**, *27*, 323.
[23] J. Kolarik, F. Lednicky, G. Locatt, L. Fambre, *Polym Eng. Sci.* **1997**, *37*, 128.
[24] E. Ivankova, R. Adhikari, G. H. Michler, R. Weidisch, K. Knoll, *J. Polym. Sci: Polym. Phys.* **2003**, *41*, 1157.
[25] I. M. Ward (Ed): "*Developments in Oriented Polymers*", Elsevier Applied Science Publishers, London 1987.
[26] G. W. Ehrenstein, Cl. Martin, *Kunststoffe* **1985**, *75*, 105.
[27] N. D. Jordan, D. C. Bassett, R. H. Olley, P. J. Hine, I. M. Ward, *Polymer* 2003, 44, 1133.
[28] R. Bjecovic, *Ph. D. Thesis*, Universität Gesamthochschule Kassel, 2003.
[29] J. Karger-Kocsis, *Polymer Eng. Sci.* **1996**, *36*, 203.
[30] G. H. Michler, R. Godehardt, *Cryst. Res. Technol.* **2000**, *35*, 863.
[31] R. Olley, D. C. Bassett, P. J. Hine, I. M. Ward, *J. Mat. Sci.* **1993**, *28*, 1107.
[32] G. H. Michler, *Phys. Stat. Soc. (a).* **1995**, *150*, 185
[33] G. H Michler, *Colloid Polym. Sci.* **1992**, *270*, 627.
[34] C. E. Schwier, A. S. Argon, R. E. Cohen, *Polymer* **1985**, *26*, 1985.
[35] R. Weidisch, G. H. Michler, in: "*Block Copolymers*", F. J. Balta´Calleja, Z. Roslaniec Eds., p. 215, Marcel Dekker, New York 2000.
[36] T. A. Huy, R. Adhikari, G. H. Michler, *Polymer* **2003**, *44*, 1247.
[37] M. Fujimora, T. Hashimoto, H. Kawai, *Rubber Chem. Technol* **1998**, *51*, 215.
[38] E. J. Kramer, In "*Advances in Polymer Science: 52/53, Crazing in Polymers-Vol I*", H. H. Kausch Ed., p. 5, Springer Verlag, Berlin, Heidelberg 1983.